Biomass Conversion and Biorefinery
https://doi.org/10.1007/s13399-024-05319-5

ORIGINAL ARTICLE

Cellulose-derived carbon aerogel from rice straw for high-performance lithium-ion battery anodes

Co D. Pham[1,2] · Khoi D. Tran[1,2] · Thanh M. Truong[1,2] · Phung K. Le[1,2]

Received: 19 October 2023 / Revised: 24 December 2023 / Accepted: 12 January 2024

Abstract

The increasing demand for energy storage solutions in recent years has driven the development of materials that are both environmentally friendly and long-lasting for battery manufacturing. As an alternative to conventional materials suffering from limited theoretical capacities, low energy densities, and a scarcity of active sites, carbon-based materials derived from wasted feedstocks such as rice straw could be regarded as a prospective precursor for the fabrication of anodes in lithium-ion batteries. Existing research concentrates on carbon materials with superior electrical conductivity and expansive specific surface areas, like graphene or carbon nanotubes. However, their intricate preparation methods, high costs, and nonrenewable nature significantly constrain their industrial-scale production and extensive use. For the first time, in this study, microfibrillated cellulose, which was extracted from agricultural waste, acted as the precursor for the synthesis of carbon aerogels through a facile route without any modification. The resulting carbon-based material exhibited an impressive initial specific charge capacity of 348.6 mAh g^{-1} and maintained a stable performance with nearly 257.5 mAh g^{-1} after over 100 cycles. These achievements not only represent a substantial advancement in the efficient utilization of agricultural waste to address environmental concerns but also introduce a valuable resource for advancing energy storage technology.

Keywords Cellulose-derived carbon aerogel · Rice straw · Lithium-ion battery

1 Introduction

In light of the escalating energy and environmental crises, the need for sustainable advancements in energy materials has become more pressing. Lithium-ion batteries (LIBs), recognized for their efficiency and eco-friendly attributes, find diverse applications due to their high energy density and robust cycle stability [1, 2]. Within LIBs, anode materials are pivotal, captivating the attention of researchers. While mainstream commercial anode material graphite offers stability with a low-voltage platform, its current capacity of 372 mAh g^{-1} falls short [3]. This limitation impedes the progression of next-generation lithium-ion batteries, demanding enhanced cathode materials with greater capacities, such as reported porous carbon materials. Addressing this challenge is crucial for the widespread application of high-energy, high-power lithium-ion batteries, urging scientists to explore novel avenues.

Carbon-based materials with high surface area, porous structures with certain electrical conductivity, high mechanical strength, and good charge-carrying capacity are increasingly being studied in energy storage applications, especially in batteries, fuel cells, and supercapacitors. These supercapacitors, fuel cells, solar cells, and other electrical energy storage devices typically require easily tunable pores, thin pore walls, large surface areas, and nanoscale structures to create favorable conditions and regulate the adsorption of charge carriers such as ions and electrons [4]. Carbon aerogels with remarkable attributes such as high porosity and astonishingly low density offer massive benefits regarding cellulose regeneration and environmental friendliness with low-carbon impact [5], coupled with their great porosity and excellent adsorption capabilities. Among the precursors for fabricating porous carbon materials utilized as anode in LIBs, cellulose aerogels can be considered a prospective candidate [6]. Leveraging cellulose aerogels as precursors

✉ Phung K. Le
phungle@hcmut.edu.vn

[1] Faculty of Chemical Engineering, Ho Chi Minh City University of Technology (HCMUT), 268 Ly Thuong Kiet Street, Ho Chi Minh City, Vietnam

[2] Vietnam National University Ho Chi Minh City, Linh Trung ward, Thu Duc District, Ho Chi Minh City, Vietnam

Published online: 23 January 2024

not only facilitates the mass production of cost-effective, environmentally friendly porous carbon-based anode materials but also addresses the shortcomings of traditional carbon materials.

For instance, Huang et al. [7] innovatively developed a three-dimensional (3D) carbonaceous foam using the aerogel structure from bacterial cellulose (BC) as a flexible framework for iron oxides in LIBs. The resulting 3D carbonized BC (CBC) exhibited remarkable electrical conductivity and mechanical stability due to its highly interconnected nanofiber structures. Employing an in situ thermal decomposition method, they precisely coated amorphous Fe_2O_3 (A-Fe_2O_3) onto CBC nanofibers. The resulting A-Fe_2O_3@CBC composite boasted a Brunauer-Emmett-Teller specific surface area of 327 m^2/g and a total pore volume of 0.59 cm^3/g. The porous structure of CBC facilitated electrolyte penetration, while the smaller pores in Fe_2O_3 enhanced the transport of lithium ions. The synergistic effect of well-dispersed Fe_2O_3 nano-shells and hierarchical pores in the A-Fe_2O_3@CBC composite demonstrated stable cycling performance and high-rate capability in a half-cell configuration, positioning it as a promising anode material for future high-performance LIB applications. Similarly, Wan et al. [8] introduced a novel flexible nano-Fe_3O_4-decorated 3D carbon nanofiber foam derived from BC, named Fe_3O_4-BC-CNFs. This material, synthesized through a hydrothermal approach followed by carbonization, exhibited exceptional mechanical stability and delivered a high reversible capacity of 754 mAh/g after 100 cycles at 100 mA/g. The superior electrochemical performance of Fe_3O_4-BC-CNFs was attributed to the highly dispersed Fe_3O_4 nanoparticles on BC/CNFs and the interconnected BC-CNFs, providing a substantial material/electrolyte contact area and promoting rapid diffusion rates of Li^+.

In a different approach by Zhou et al. [9], Si nanoparticles and graphite micro-sheets (GMs) were meticulously assembled on TEMPO-oxidized BC (TOBC) foams through molecular engineering to create robust and flexible LIB electrode materials. The resulting GM/TOBC/Si nanomat exhibited interconnected porous channels, fostering a bicontinuous electron and ion mechanism for electrochemical kinetics. Additionally, GM, obtained through facile micromechanical exfoliation, securely adhered to the surface of Si nanoparticles via electrostatic attraction, ensuring significant electrical conductivity throughout the entire electrode. Leveraging these advantages, the collector-free GM/TOBC/Si nanomat anode demonstrated superior cycle life (639.4 mA h/g after 400 cycles at 1.0 A/g) and rate capability (298.6 mA h/g at 1.6 A/g). However, despite the advancements in existing research focusing on carbon materials with superior electrical conductivity and expansive specific surface areas, such as graphene or carbon nanotubes [10], their complex preparation methods, high costs, and nonrenewable nature significantly impede their industrial-scale production and widespread use. Consequently, the development of a new and straightforward route to produce anode material in batteries plays a crucial role in advancing sustainability.

The introduction of nitrogen-doped carbon materials as conductive networks is suggested to augment the concentration of free electrons within the anode material, resulting in enhanced performance in LIBs. Nitrogen doping assumes a pivotal role in broadening the energy band gap, adjusting conductivity type, modifying the electronic structure, and amplifying the free carrier density of graphene. Consequently, the incorporation of nitrogen doping exhibits significant potential for effectively improving conductivity and stability, thereby substantially elevating the overall anode performance in LIBs [11]. In order to assess the performance of carbon cellulose aerogel in lithium-ion batteries, rice straw was employed to produce micro-fibrillated cellulose (MFC), serving as the precursor for fabricating carbon aerogels. The process without any modification or graphitization involved the use of polyamide epichlorohydrin resin (PAE) as the cross-linker to possess a nitrogen-containing group in the structure of anode material for the first time. The structure of obtained materials was characterized using Fourier-transform infrared spectroscopy (FTIR), powder X-ray diffraction (PXRD), and scanning electron microscopy (SEM) coupled with energy-dispersive X-ray analysis (EDX). Charge-discharge experiments were carried out to assess the suitability of these materials as anodic electrodes in LIBs.

2 Experimental section

2.1 Materials

Rice straw (RS) was harvested from An Giang province, Viet Nam. All chemicals employed in this work including sodium hydroxide (NaOH, purity of 96%), hydrogen peroxide (H_2O_2, 30 wt%), sulfuric acid (H_2SO_4, 98 wt%), and polyamide-epichlorohydrin resins (PAE, 12.5 wt%) were purchased and used without any purification.

2.2 Methods

The rice straw was grounded, and then treated with NaOH 6 wt% at a liquid-to-solid ratio of 20:1 in 2 h, at 80 °C. The obtained slurry was rinsed with reverse osmosis water (RO) until it acquired a neutral pH value. Afterward, the system was then mixed with a mixture of 10 wt% H_2O_2 and 0.5 wt% NaOH solutions at 80 °C for 1 h. The ratio of the liquid mixture to powder was 20:1 (mL:g). The obtained powder was washed with RO water until pH-balanced before drying in an oven at 80 °C overnight. The obtained cellulose was

hydrolyzed with 40 wt% H_2SO_4 at 45 °C for 1 h. The hydrolysis step was terminated by adding water. The suspension was settled down over time and then the upper layer of water was removed from the suspension prior to introducing fresh distilled water into the residue until the suspension reached neutral pH. After that, the entire mixture was homogenized for 2 h at 15000 rpm to finally achieve the micro-fibrillated cellulose (MFC) suspension.

A mixture of an aqueous suspension of MFC (1 wt%) and PAE 60 wt% was vigorously agitated for 15 min. The suspension was then poured into a stainless-steel mold. Next, the sample is frozen in liquid nitrogen to obtain the hardened form, followed by freeze-dried by Toption TPV-50F lyophilizer under vacuum conditions for 48 h. Finally, the MFC aerogel (MFCA) was yielded via a heat-annealing process at 120 °C for 3 h. The cellulose aerogel after drying undergoes carbonization. The aerogel is heated in a furnace in an anaerobic environment at 500 °C for 2 h to achieve carbon cellulose aerogel (C-MFCA). The scheme describing the synthesis process for C-MFCA is illustrated in Fig. 1.

2.3 Characterization

Fourier-transform infrared spectroscopy (FTIR) analysis was executed on a Bruker Tensor 37 spectrometer, and each spectrum was recorded in the 4000–500 cm^{-1} range. The structural characteristics of the samples were studied using an SEM Prisma E with a 10-kV operation voltage. The nitrogen adsorption-desorption isotherms and various parameters for each specimen were determined on Nova Station A 2200e–Quantachrome using the Brunauer-Emmett-Teller (BET) equation and Barret-Joyner-Halenda (BJH) techniques from the equipment software. Prior to the measurements, the specimens undergo degassing in a vacuum at 120 °C for 4 h to eliminate trapped gases. PXRD analyses were performed on the Bruker Advance D8 Diffractometer (Bruker AXS, Germany), which was equipped with monochromatized Cu-Ka radiation (k = 1.5418 A°), operated at 40 kV and 40 mA, room temperature. The data were collected in the 2q range of 2°–30° with a scan rate of 0.6° min^{-1} and a step size of 0.01°. The index of crystallinity of samples after each step was calculated using the following equation:

$$CrI = \frac{I_{002} - I_{am}}{I_{002}} \times 100\% \quad (1)$$

in which CrI is the crystallinity index, I_{002} is the maximum intensity of 002 lattice diffraction, and I_{am} is the intensity of diffraction at 2θ = 18°.

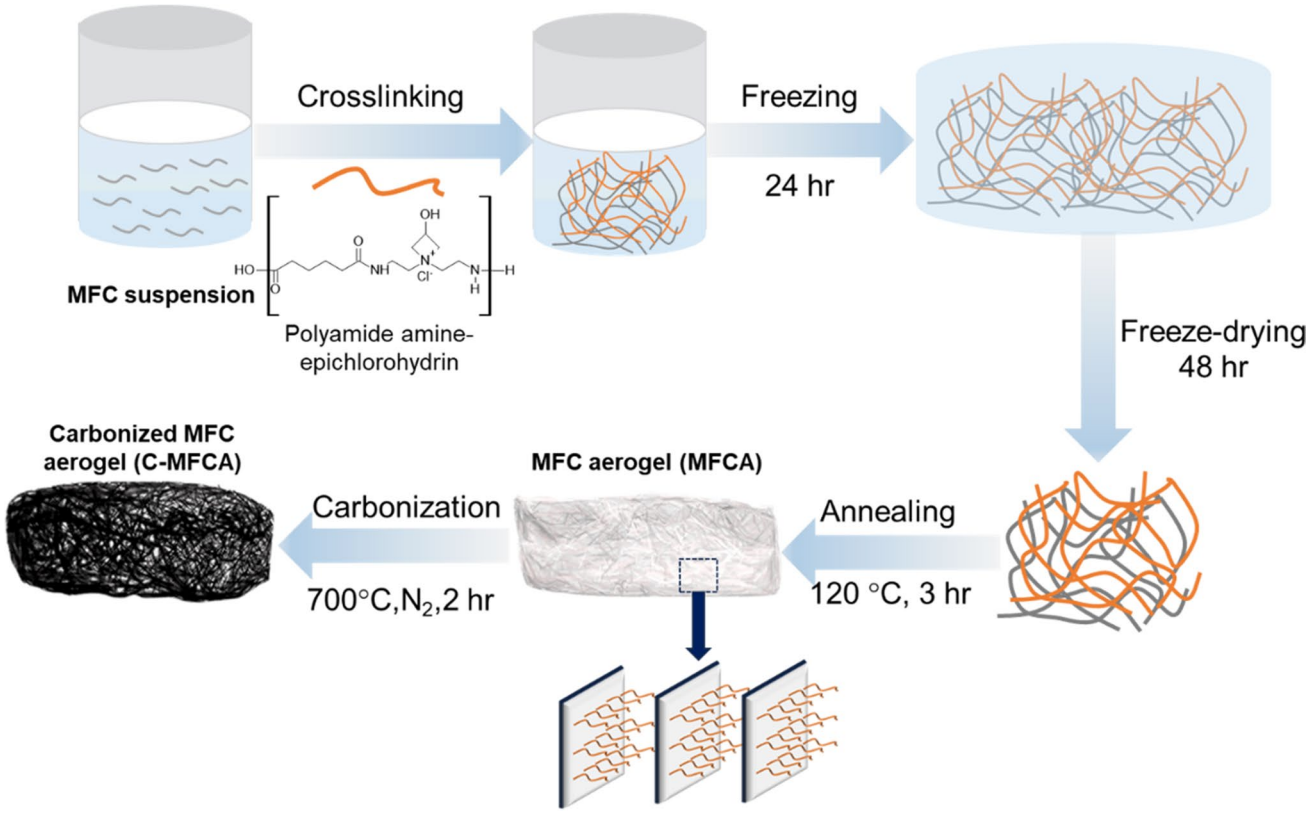

Fig. 1 Schematic for synthesizing MFC carbon aerogel

The bulk density of each MFC aerogel is calculated through its weight and volume. The porosity (φ) is determined using the bulk density (ρ_α) and the average skeletal density of components (ρ_b) as shown in the equation below:

$$\varphi = \left(1 - \frac{\rho_\alpha}{\rho_\beta}\right) \times 100\% \quad (2)$$

The average skeletal density ρ_β of the cellulose composite was given by:

$$\rho_b = \frac{1}{\frac{W_{cellulose}}{\rho_{cellulose}} + \frac{W_{PAE}}{\rho_{PAE}}} \quad (3)$$

where $W_{\text{cellulose}}$ and W_{PAE} are weight fractions of cellulose and PAE, respectively. The skeletal density of PAE (ρ_{PAE}) is assumed as 1.150 mg/cm^3 while that of cellulose ($\rho_{\text{cellulose}}$) is taken as 1.45 mg/cm^3.

The electrochemical performance of a CR2032 coin-type battery was examined. The CR2032-type coin cells were built in an argon-filled glove box (MBRAUN) with less than 1 ppm water and oxygen concentration. The electrodes were made on Cu foils using slurries containing 70% active material (carbon aerogel), 15% Super P, which is conductive carbon black, and 15% poly (acrylic acid) binder in ethanol solvent. The slurry was spread over Cu foil and dried for 3 h in an oven then overnight in a vacuum oven at 70 °C. The anode materials were cut into 15-mm-diameter circles. The cells were built with lithium foil as the counter electrode, Celgard 2400 as the separator, and 1 M $LiPF_6$ in ethylene carbonate (EC) and diethylene carbonate (1:1 in volume) as the electrolyte. The discharge/charge tests were performed using a battery cycler system with a voltage range of 0.01–3.00 V at 1C (Arbin Instruments, BT2143).

3 Results and discussions

Figure 2 shows XRD result for rice straw, cellulose, and micro-fibrillated cellulose (MFC). With an amorphous wide hump and crystalline sharp peaks, these patterns are typical of semi-crystalline materials. There is a preponderance of type I cellulose in all of the diffractogram profiles, as evidenced by the presence of peaks at around 2q =15° (plane 101), 18° (plane 101), 23° (plane 200), and 34.5° (plane 004). It can be observed that the CrI value rose after each step. With a crystalline index (CrI) of 36%, rice straw has poor crystallinity. CrI increases considerably after alkalinization and bleaching to 67.87% due to the elimination of lignin, hemicellulose, and a portion of amorphous cellulose regions.

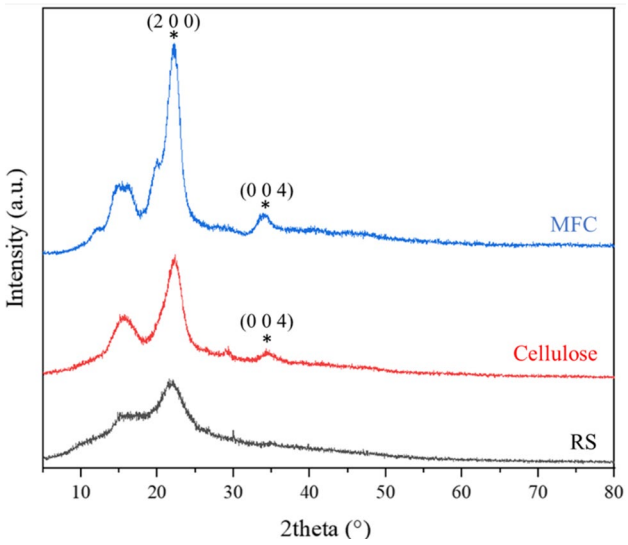

Fig. 2 PXRD pattern of rice straw, cellulose from rice straw, and microfibrillated cellulose

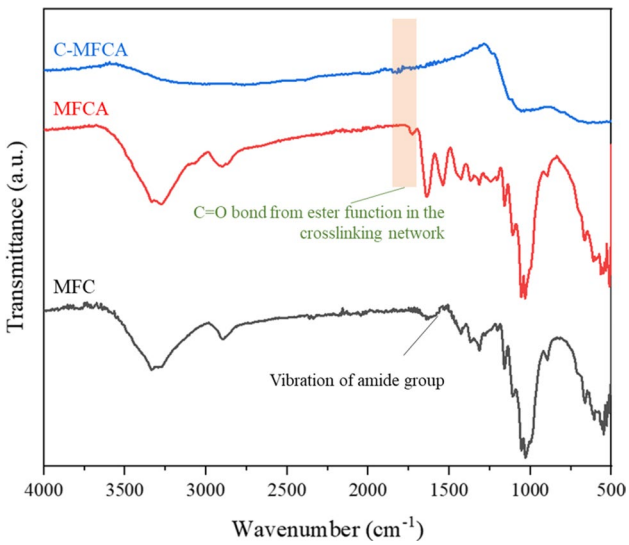

Fig. 3 FT-IR spectra of MFC, MFCA, and C-MFCA

The FTIR spectra of MFC, MFCA, and C-MFCA are shown in Fig. 3. As expected, the difference among these samples suggests that there are chemical differences between them before and after aerogel synthesis due to the presence of PAE. Specifically, the peak at 1061 cm^{-1} is caused by the C–O–C (pyranose ring) stretching of cellulose and C–H rock vibrations. Both the FTIR spectra of MFC and MFCA contain broad peak bands at wave number 3344 cm^{-1}, which correspond to O–H stretching vibrations. The C–H and C–O bond vibrations in the cellulose polysaccharide ring correspond to a wavenumber of 1368 cm^{-1}. Especially, the

observed differences are 1630 cm^{-1} peak which represents the amide group vibration of PAE and 1724 cm^{-1} which represents C=O bond from the ester function in the cross-linking network [12]. Through undergoing the heating and drying process, the active azetidinium establishes covalent bonds with carboxyl groups on fibers. Simultaneously, cross-links form within and between PAE chains and strong hydrogen bonds as reported in previous studies [13–15]. Therefore, a network of cross-linked polymers is created, linking the surfaces of adjacent fibers (Fig. 4). Besides, after the carbonization process, the obtained material exhibited distinct structural characteristics compared to its initial structure. As can be seen, a slight peak around 1600 cm^{-1} in C-MFCA corresponds to the presence of highly conjugated C=O bonds, signifying the altered structure of the carbohydrate during the process.

Figure 5 provides details regarding the structure of MFCA and C-MFCA. Initially, the majority of PAE-MFC clusters in MFCA had a diameter ranging from 10 µm to nearly 40 µm. After the carbonization process, the diameter of these clusters drastically reduced to 3–6 µm, leaving void space for wider pores with pore sizes ranging from 10 to 20 µm. In C-MFCA, cellulose microfibers are still bound together via thin PAE films through robust hydrogen bonding, resulting in a porous structure with interconnected three-dimensional patterns.

After the carbonization process, there was a rise in the porosity of carbon aerogel, resulting in the decreased bulk density of the material. Regarding the elemental composition, the nitrogen content in C-MFCA is significantly higher when compared to this value in MFCA (Table 1). Due to the restructuring and diminishment of some functional groups in the structure of MFCA during the carbonization process (oxygen-containing group), the N percentage increased and accounted for 10.49 wt% with better distribution in C-MFCA (Fig. 6), which has a great potential for lithium-ion battery.

Figure 7 illustrates the charge-discharge behavior of the anode-based C-MFCA at 1C for the 1st, 2nd, and 100th cycle. During the initial cycle, the anode fabricated from C-MFCA exhibited discharge plateau slopes at around 0.5–0.7 V, indicating the formation of the solid electrolyte interface (SEI) layer (Fig. 8). While this layer is essential for battery stability, an excessively thick or poorly formed SEI layer could increase internal resistance, limit ion diffusion, and hamper the overall electrochemical performance of the electrode [16]. In this situation, the anode displayed a robust

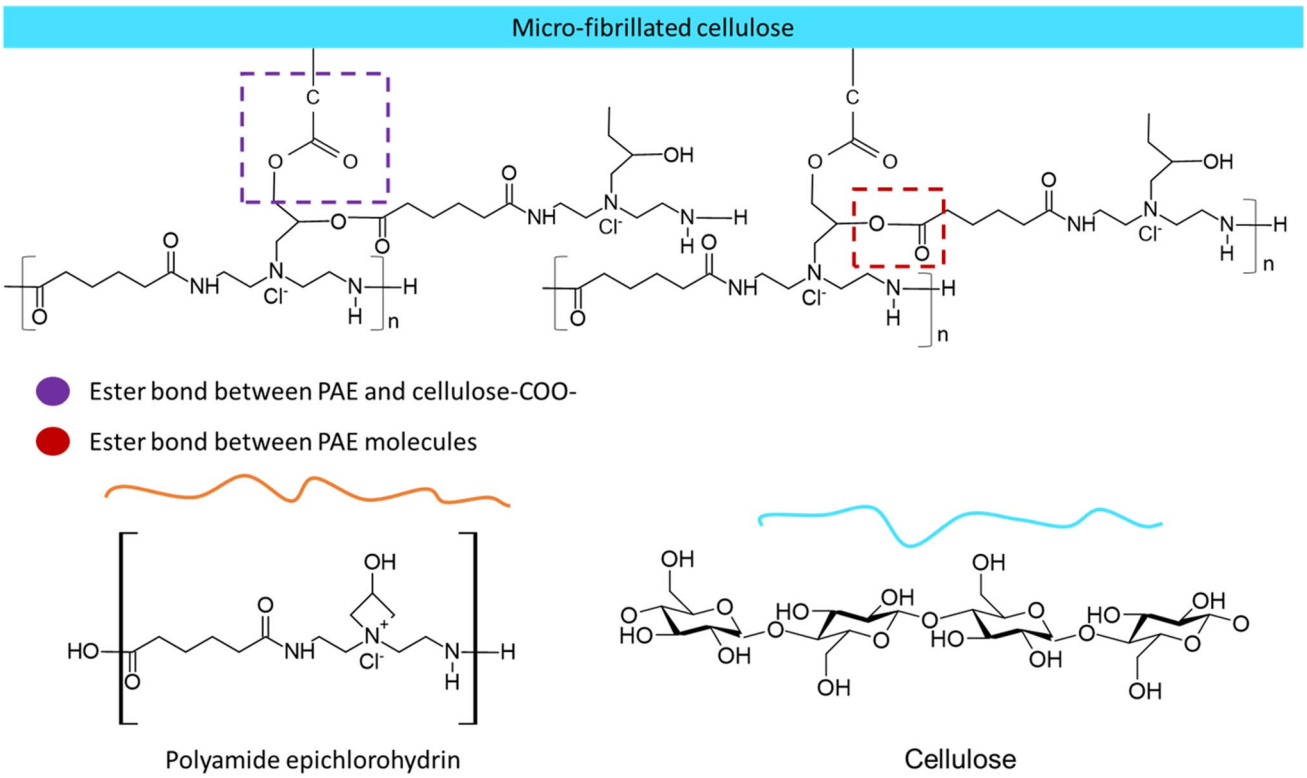

Fig. 4 The proposed bonding of PAE and MFC in the aerogel matrix

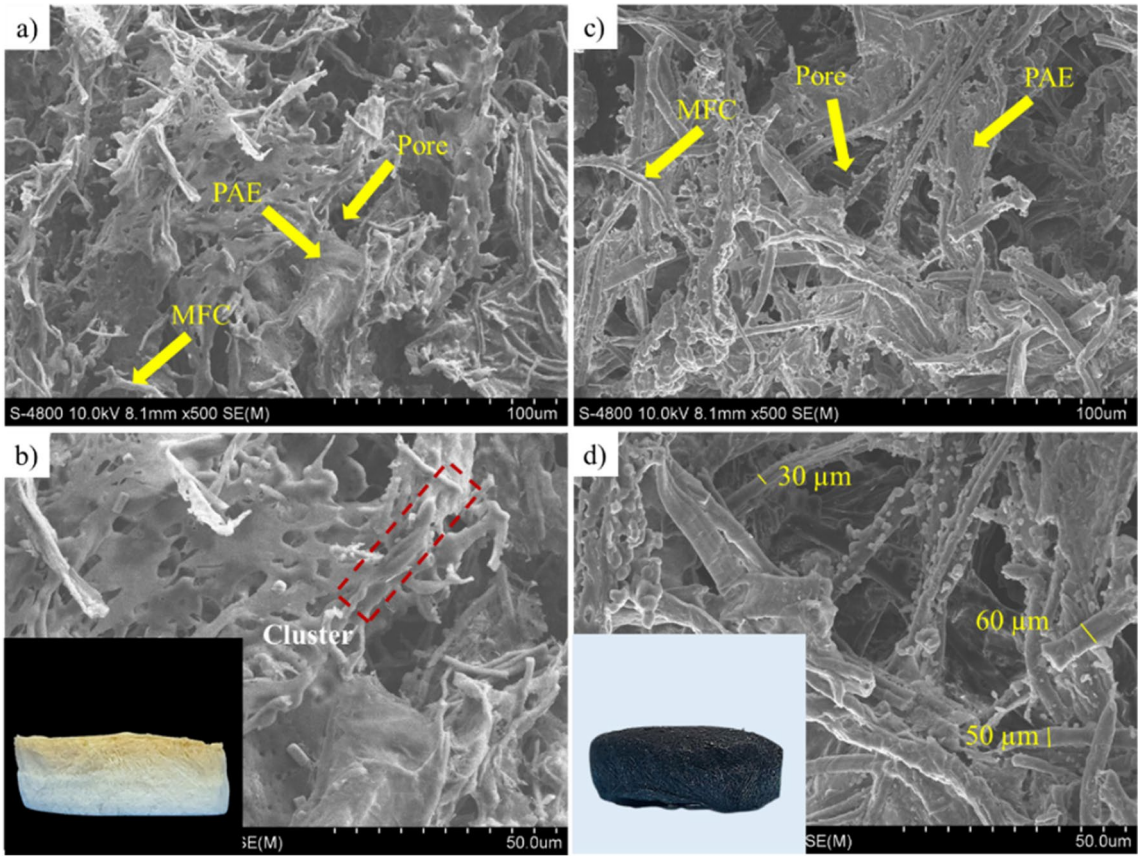

Fig. 5 SEM image of MFCA (**a**, **b**) and C-MFCA (**c**, **d**)

Table 1 The comparison of the elemental composition and porosity of CA and CCA

	MFCA	C-MFCA
Elemental analysis		
C wt%	51.54	58.12
O wt%	40.15	31.39
N wt%	8.31	10.49
Porosity analysis		
Bulk density (g cm^{-3})	0.0396 ± 0.0001	0.0260 ± 0.0008
Porosity (%)	96.88 ± 0.010	98.52 ± 0.047
SBET (m^2/g)	36.61	60.06
Total pore volume (cm^3/g)	0.0624	0.0681

charge capacity of 348.6 mAh g^{-1}, with a corresponding discharge capacity of 317.9 mAh g^{-1} and an initial Coulombic efficiency of nearly 80%. By the second cycle, the charge and discharge capacities decreased to 279.5 mAh g^{-1} and 276.3 mAh g^{-1}, respectively.

Remarkably, after 100 cycles, the porous carbon-based anode material still maintained a specific capacity of 254.8 mAh g^{-1}, demonstrating an outstanding capacity retention rate of 97.9% as shown in Fig. 9. In the context of lithium battery discharge, the specific capacity signifies the material capacity for lithium-ion alloying, while the charging capacity reflects the reversible stripping capacity of Li^+. A higher coulombic efficiency indicates minimized Li^+ loss and irreversible capacity during charging and discharging [17, 18]. The carbon-based anode material, derived from cellulose aerogel carbonization, exhibited impressive charge-discharge capacity and Coulombic efficiency. This outcome indicates excellent Li^+ imbibition in the prepared material, attributed to the enhanced Li^+ transmission rate facilitated by the three-dimensional porous structure. With the greater nitrogen content and better porosity, the complete reaction of Li^+ at the electrode/electrolyte interface significantly enhanced the cycling stability of the electrode material to overcome the pulverization as shown in Fig. 8. Previous studies found that active material particles in the electrode undergo mechanical fragmentation due to repeated charge-discharge cycles. This phenomenon occurs particularly in electrodes made of silicon [19], which expand and contract significantly during cycling. Using the carbon-based material as a buffer layer

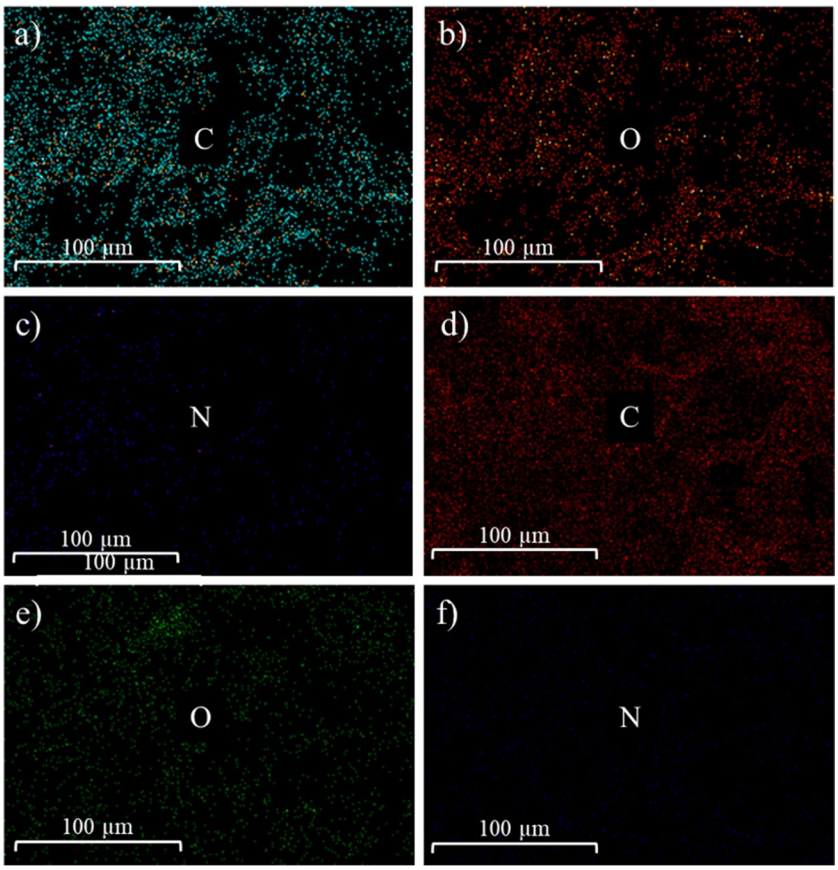

Fig. 6 The EDX-mapping result of carbon, oxygen, and nitrogen in MFCA (**a**, **b**, **c**) and C-MFCA (**d**, **e**, **f**)

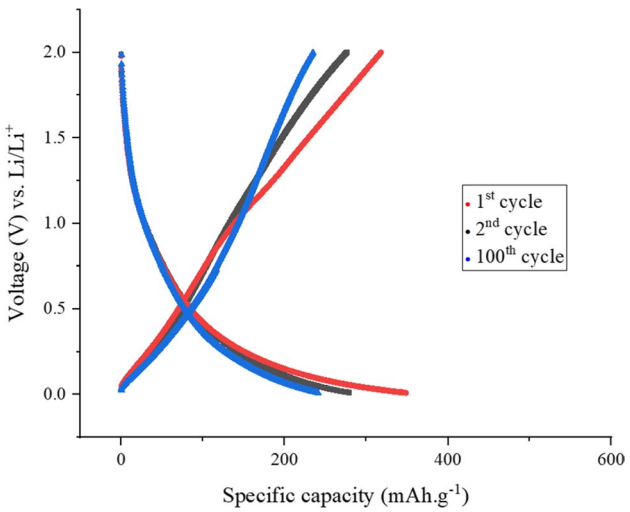

Fig. 7 Galvanostatic charge–discharge profile for C-MFCA at 1C at the 1st, 2nd, and 100th cycle

improves the durability and provides large volume vibration to overcome the loss of electrical contact, capacity, and the degradation of battery performance over time.

The evaluation of the electrochemical performance of various electrode materials, including additional anode materials, is listed in Table 2. The anode materials fabricated in this study demonstrated significantly enhanced capacity with a simple production process. This improvement in electrochemical performance can be attributed to the large specific surface area, great porosity, and well-connected conductive networks, all of which facilitate efficient lithium reactions.

4 Conclusions

In this study, rice straw produced during agricultural production was utilized in the synthesis of C-MFCA through a cross-linking and carbonization method. Following the pyrolysis phase, the obtained material shows distinct structural characteristics. Analysis using FTIR, XRD, and SEM-EDX indicated the presence of a crystalline structure of cellulose, with a high nitrogen content of 10.49 wt%. In the context of battery electrode fabrication, the C-MFCA exhibited superior stability compared to massive works in the past when graphite and metal-containing composites were used as anodes in lithium-ion batteries. Specifically,

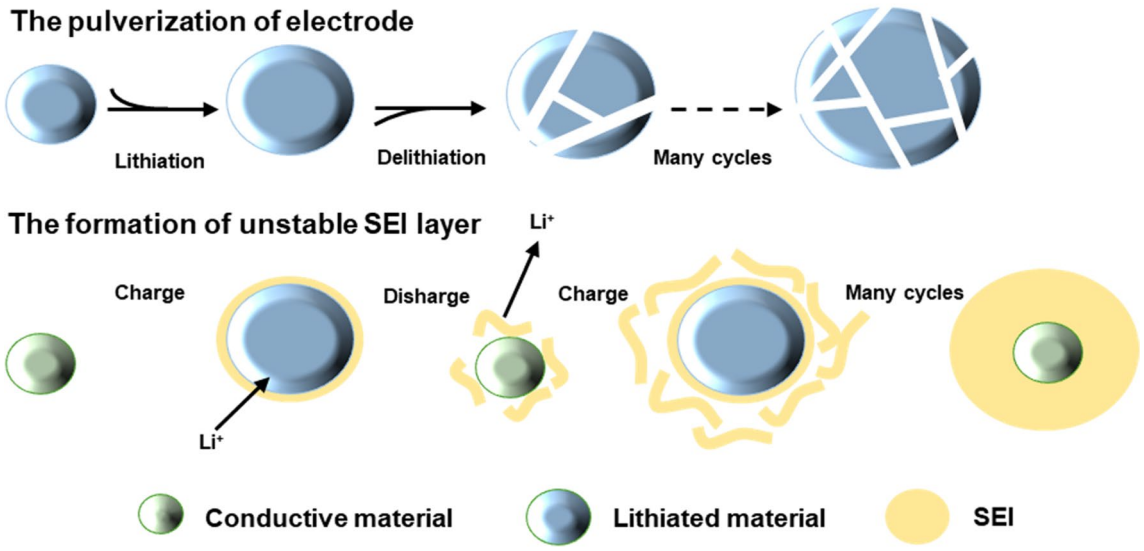

Fig. 8 The pulverization and SEI formation in lithium-ion battery

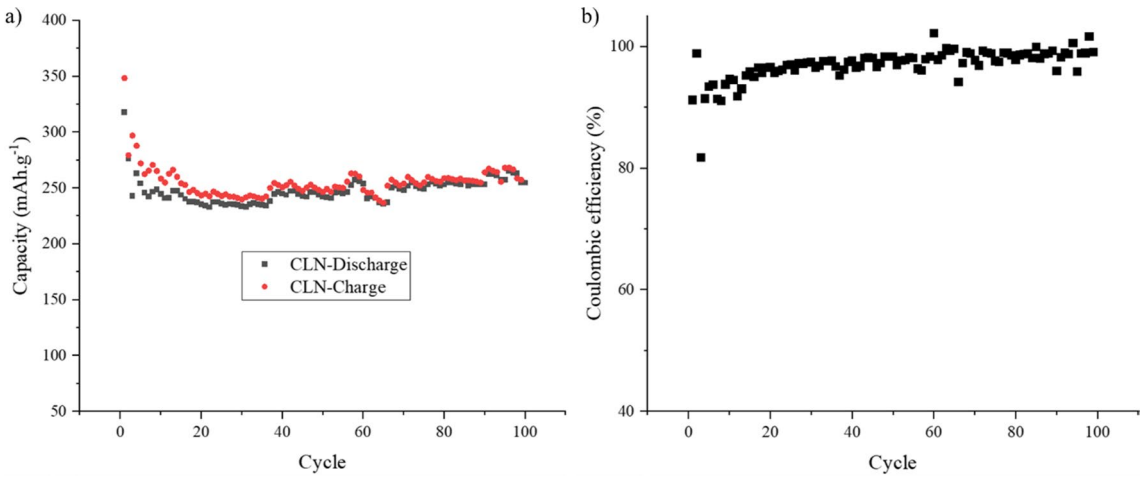

Fig. 9 Cycle performance of C-MFCA samples at 1C after 100 cycles

Table 2 The comparison of the performance of various materials from previous research as the anode in the LIBs

Anode material	Nitrogen-doped graphene	SnO_2@C	TiO_2 nanofibers	C-MFCA
Specific charge capacity (mAh g^{-1}) at 1C	230	450	150	257.5
Cycle number	100	50	50	100
Reference	[20]	[21]	[22]	This work

the C-MFCA displayed an impressive initial lithiation-specific capacity of up to 348.6 mAh g^{-1} and maintained a stable reversible capacity of 257.5 mAh g^{-1}. Consequently, this research not only underscores the considerable potential of these carbon-based materials in electrochemical applications but also presents a novel solution to environmental remediation challenges. With the growing energy demands, this study also demonstrates a pathway for the effective utilization of rice straw in the realm of energy storage devices, particularly lithium-ion batteries.

Acknowledgements We acknowledge the support of time and facilities from Ho Chi Minh City University of Technology (HCMUT), VNU-HCM for this study.

Author contribution Co D. Pham: conceptualization; data curation; writing—original draft; review and editing; formal analysis; investigation; visualization. Khoi D. Tran: investigation; writing—original draft. Thanh M. Truong: methodology, supervision, review, and editing. Phung K. Le: funding acquisition, methodology, project administration, resources, supervision, review, and editing. The manuscript was written through the contributions of all authors. All authors have given approval to the final version of the manuscript.

Funding This research is funded by Vietnam National University Ho Chi Minh City (VNU-HCM) under grant number 562-2022-20-04.

Data availability The datasets generated during the current study are available from the corresponding author on reasonable request.

Declaration

Ethical approval Not applicable

Competing interests The authors declare no competing interests.

References

1. Li W, Linze H, Pei Z (2022) Preparation of high cycle performance carbon-based anode materials based on cellulose aerogels for lithium-ion batteries. Int J Electrochem Sci 17(6):220625. https://doi.org/10.20964/2022.06.10
2. Zhu J, Su Z (2018) Synthesis and electrochemical characteristics of Li3V2(PO4)3/C as a novel Li-ion battery cathode material. Int J Electrochem Sci 13(3):3063–3069. https://doi.org/10.20964/2018.03.37
3. Yi C, Yang Y, Zhang T, Wu X, Sun W, Yi L (2020) A green and facile approach for regeneration of graphite from spent lithium ion battery. J Clean Prod 277:123585. https://doi.org/10.1016/j.jclepro.2020.123585
4. Karamveer Sheoran VK, Thakur, Siwal SS (2022) Synthesis and overview of carbon-based materials for high performance energy storage application: a review. Mater Today Proc 56:9–17. https://doi.org/10.1016/j.matpr.2021.11.369
5. Do NHN et al (2020) Advanced fabrication and application of pineapple aerogels from agricultural waste. Mater Technol 35(11–12):807–814. https://doi.org/10.1080/10667857.2019.1688537
6. Lv Y et al (2021) Efficient adsorption of diclofenac sodium in water by a novel functionalized cellulose aerogel. Environ Res 194:110652. https://doi.org/10.1016/j.envres.2020.110652
7. Huang Y et al (2016) Amorphous Fe2O3 nanoshells coated on carbonized bacterial cellulose nanofibers as a flexible anode for high-performance lithium ion batteries. J Power Sources 307:649–656. https://doi.org/10.1016/j.jpowsour.2016.01.026
8. Wan Y, Yang Z, Xiong G, Luo H (2015) A general strategy of decorating 3D carbon nanofiber aerogels derived from bacterial cellulose with nano-Fe_3O_4 for high-performance flexible and binder-free lithium-ion battery anodes. J Mater Chem A Mater 3(30):15386–15393. https://doi.org/10.1039/C5TA03688G
9. Zhou X et al (2019) Layer-by-layer engineered silicon-based sandwich nanomat as flexible anode for lithium-ion batteries. ACS Appl Mater Interfaces 11(43):39970–39978. https://doi.org/10.1021/acsami.9b13353
10. Pham CD et al (2023) The utilization of black liquor from rice straw pretreatment stage on the syntheses of carbon-based materials using in anodes ion-lithium batteries production. J Mater Sci Mater Electr 34(4):335. https://doi.org/10.1007/s10854-023-09840-7
11. Witjaksono G et al (2021) Effect of nitrogen doping on the optical bandgap and electrical conductivity of nitrogen-doped reduced graphene oxide. Molecules 26(21):6424. https://doi.org/10.3390/molecules26216424
12. Yang W, Bian H, Jiao L, Wu W, Deng Y, Dai H (2017) High wet-strength, thermally stable and transparent TEMPO-oxidized cellulose nanofibril film via cross-linking with poly-amide epichlorohydrin resin. RSC Adv 7(50):31567–31573. https://doi.org/10.1039/C7RA05009G
13. Nguyen L et al (2022) Microfibrillated cellulose from pineapple leaves for synthesizing novel thermal insulation aerogels. Chem Eng Trans 97:61–66. https://doi.org/10.3303/CET2297011
14. Obokata T, Isogai A (2007) The mechanism of wet-strength development of cellulose sheets prepared with polyamideamine-epichlorohydrin (PAE) resin. Colloids Surf A Physicochem Eng Asp 302(1–3):525–531. https://doi.org/10.1016/j.colsurfa.2007.03.025
15. Yang D, Sotra A, Pelton RH (2019) Switching off PAE wet strength. Nord Pulp Paper Res J 34(1):88–95. https://doi.org/10.1515/npprj-2018-0074
16. Mao C et al (2018) Balancing formation time and electrochemical performance of high energy lithium-ion batteries. J Power Sources 402:107–115. https://doi.org/10.1016/j.jpowsour.2018.09.019
17. Lin X, Khosravinia K, Hu X, Li J, Lu W (2021) Lithium plating mechanism, detection, and mitigation in lithium-ion batteries. Prog Energy Combust Sci 87:100953. https://doi.org/10.1016/j.pecs.2021.100953
18. Zhang W-J (2011) Lithium insertion/extraction mechanism in alloy anodes for lithium-ion batteries. J Power Sources 196(3):877–885. https://doi.org/10.1016/j.jpowsour.2010.08.114
19. Yu Z, Cui L, Zhong B, Qu G (2023) Research progress on the structural design and optimization of silicon anodes for lithium-ion batteries: a mini-review. Coatings 13(9):1502. https://doi.org/10.3390/coatings13091502
20. Liu H et al (2021) Characteristics and electrochemical performances of nitrogen-doped graphene prepared using different carbon and nitrogen sources as anode for lithium ion batteries. Int J Electrochem Sci 16(4):210459. https://doi.org/10.20964/2021.04.03
21. Liu L, Li M, Sun Y, Ma M, Yang X, Wang H (2022) SnO2@C composite as anode material of lithium-ion batteries with enhanced cycling stability. Int J Electrochem Sci 17(3):22031. https://doi.org/10.20964/2022.03.20
22. Li J et al (2016) Facile approach to prepare TiO2 nanofibers via electrospinning as anode materials for lithium ion batteries. J Mater Sci : Mater Electr 27(8):8682–8687. https://doi.org/10.1007/s10854-016-4889-3